

Toughening Effects of Interleaved Nylon Veils on Glass Fabric/Low-Styrene-Emission Unsaturated Polyester Resin Composites

Kieran O'Donovan, Dipa Ray, Michael A. McCarthy

Mechanical, Aeronautical and Biomedical Engineering Department, Irish Centre for Composites Research (ICOMP), Materials and Surface Science Institute, University of Limerick, Limerick, Ireland

Correspondence to: D. Ray (E-mail: Dipa.Roy@ul.ie)

ABSTRACT: The effectiveness of using interleaved nylon veils to increase the interlaminar toughness of glass fiber reinforced, low-styrene emission unsaturated polyester resin composites has been investigated. Samples were manufactured by a hand lay-up technique followed by compression moulding. Nylon 66 veils were used, with the veil content varying from 0% to 4% by weight. Double cantilever beam, short beam shear, and three point bend tests were performed. The increasing levels of nylon veil content improved the interlaminar toughness of the composites, which was characterized by critical strain energy release rate (G_{IC}). The maximum G_{IC} for crack propagation of a nylon interleaved composite increased by almost 170% over the baseline glass fiber reinforced composite. Dynamic Mechanical Analysis revealed an increase in the damping parameter of up to 117%. Image analysis via Digital Image Correlation and Scanning Electron Microscopy revealed increased fiber bridging between adjacent plies as a key reason for these improvements. © 2014 Wiley Periodicals, Inc. *J. Appl. Polym. Sci.* **2015**, *132*, 41462.

KEYWORDS: composites; fibers; mechanical properties

Received 24 April 2014; accepted 25 August 2014

DOI: 10.1002/app.41462

INTRODUCTION

Glass fiber reinforced composite materials are used in a wide range of applications in the automotive, consumer goods, marine, wind energy, and construction industries. For some applications, such as car bumpers, helmets, armour, etc., the most important material requirement is the capacity to absorb mechanical energy under impact conditions, before reaching complete fracture. While there are several possible energy dissipation mechanisms in composites such as fiber fracture, matrix cracking, fiber/matrix debonding, and fiber pullout from the matrix, most are not fully exploited under impact loading, without specialized structural design (e.g. crash tubes, sine wave beams etc. which can set up a stable crush zone, inducing numerous fiber fractures). The exception is delamination of adjacent plies in a laminate, which can absorb significant energy under impact conditions even if structural configurations are not optimized for energy absorption (e.g. flat plates).¹ Hence, interlaminar fracture toughness is an important property of composite laminates to be used in energy-absorption applications.

The relationship between interlaminar fracture toughness and energy absorption under impact is in fact not entirely straightforward. Various authors have shown that there exists an optimum level of fracture toughness for maximum energy

absorption under impact, and that very high interlaminar fracture toughness, such as is found in some thermoplastic composites, can result in reduced impact energy absorption, as delamination is inhibited and the delaminated area reduces.^{1–3} However, for the relatively brittle interlaminar interfaces found in most thermoset composites, this is not a consideration since the fracture toughness is well below the optimum level, and methods to increase fracture toughness are desirable, if the proposed application requires energy absorption under impact.

In this article we examine thermoset glass composites made with low-styrene emission grades of unsaturated polyester resin. Unsaturated polyester resins are generally mixed with styrene to reduce their viscosity. However, the emission of styrene during processing is a significant hazard in the workplace, and various methods of reducing such emissions have been developed, resulting in so-called "low-styrene emission" grades of resin. In these resins, additives are included which migrate to the surface to form a film, limiting styrene emission. The use of such resins is desirable from a health and safety viewpoint. Baley et al.⁴ carried out a study on the mechanical properties of composites based on low styrene emission polyester resins for marine applications. It was apparent from their study that the resin formulations proposed to limit styrene emission were significantly more brittle than those resins traditionally employed for

boat-building. Perrot et al.⁵ studied the damage behavior of glass fiber reinforced, low styrene emission polyester resin composites. They found that these resins, which have lower molecular weight than their traditional counterparts, were all quite brittle. This resulted in significantly lower composite damage resistance than composites made with traditional resins. They observed easier damage initiation and propagation for the reduced styrene matrix composites and extensive damage zones following drop weight impact tests. It is thus desirable to find ways to improve the impact resistance of composites made with low-styrene emission resins, so that they can be more widely used.

A method of controlling delamination and increasing the interlaminar toughness, which is popular in many aerospace applications, is to use interleaving thermoplastic films. Most studies in the field of interleaved composites to date have been focused on carbon fiber reinforced plastic (CFRP) composites. Lee et al.⁶ proposed an interlayer hybrid concept with nonwoven carbon tissue as a toughening and strengthening technique for conventional carbon and glass fiber-reinforced plastic laminates. The longitudinal tensile Young's modulus and strength of the hybrid specimens were lower than those of the CFRP specimen, but the transverse tensile Young's modulus and strength of some of the hybrid specimens was higher than those of the CFRP specimen, and the strength scattering of hybrid specimens was smaller than that of the CFRP specimen. Kuwata et al.⁷ investigated the interlaminar toughness of CFRP laminates, interleaved with fine, low areal weight, nonwoven veils. Five types of veils were used: two variants of polyester/carbon fiber hybrid (Hyb1 and Hyb2), and veils based on carbon, polyester (PE), and polyamide (PA) fibers. The introduction of veils resulted in a significant increase in toughness in the Mode-I loading mode. The mechanism of toughening was tentatively linked to fiber bridging effects that were enhanced by the introduction of the veils, and tough thermoplastic fibers appeared to be more effective as veil fibers than stiff carbon fibers. Kuwata et al.⁸ also investigated the mode II interlaminar toughness of the same interleaved composites and observed a significant improvement. The toughening mechanism in Mode-II appeared to be more complex, less dependent on fiber bridging and more influenced by the properties of the resin. Hamer et al.⁹ investigated CFRP laminates interleaved with laboratory-scale electrospun nylon 66 nanofibrilmat and spun-bonded nonwoven mats. They evaluated the effect of the nanoscale fibers on the fracture toughness of the composite under pure Mode I loading. It was found that the nanofibrilmat led to a major interlaminar fracture toughness improvement, as high as 255–322%, compared to a noninterleaved CFRP reference laminate. They suggested that a combination of two interlayer fracture mechanisms was responsible: the presence of bridging thermoplastic nanofibers, and the generation of a plastic zone near the crack tip. Tzetzis^{10,11} used interleaving veils to improve the toughness of the bond line in vacuum infused repairs of carbon fiber composites. The brittle resin used to infuse a repair patch was toughened by the use of fine fiber veils introduced at the bond line, between the repair patch and the substrate material, prior to the infusion process. The mode-I fracture toughness of the repair was measured by a

Double Cantilever Beam (DCB) test. Carbon fiber veils, polyester fiber veils and combinations of the two were used. It was found that the veils did not impede the production of high quality repairs and that bridging effects introduced by the veils resulted in a substantial increase in the bond line fracture toughness (initiation G_{IC} increased from 0.13 to over 0.9 kJ/m²). The most effective veil was the combination of a double layer of polyester fibers with a central carbon fiber layer.

Interleaved glass fiber reinforced plastic (GFRP) composites have been studied by only a few researchers. Yasaee et al.¹² investigated the interaction of propagating interlaminar cracks with embedded strips of interleaved materials in E-glass/epoxy composites. Interlayer strips were placed ahead of the crack path in the mid-plane of DCB specimens. Interleaving materials investigated included thermoplastic films, thermoplastic particles, chopped fibers, E-glass/epoxy prepreg strips cut to size, thermoset adhesive films and thermoset adhesive particles. The same authors investigated the Mode II interfacial toughening through these discontinuous interleaves.¹³ They concluded that the increased interply thickness from the use of an interleaved layer contributed only a small amount to the energy absorption under Mode I fracture, but was a big factor in Mode-II failure because of the introduction of more tortuous crack paths. For Mode-I fracture, maintaining a mechanical linkage between the two crack interfaces via the use of inserted fibers or films was the most effective way of increasing the Mode-I fracture toughness.

In the present study, a low styrene emission grade of unsaturated polyester resin has been selected as the matrix material, and an interleaving technique has been adopted to investigate if the interlaminar fracture toughness of the GFRP composite made with this resin can be improved. Composite panels were manufactured by hand layup with varying levels of nylon veils, followed by compression moulding. Specimens from the panels were then examined through short-beam shear (SBS) tests, three point bend (3PB) tests, double cantilever beam (DCB) tests, and dynamic mechanical analysis (DMA). The fracture surfaces were examined under scanning electron microscope (SEM).

EXPERIMENTAL

Materials

The composite panels were manufactured using Crystic 2-446PA, a room temperature curing, low styrene emission unsaturated polyester resin from Scott Bader. Butanox LPT-IN (Akzo Nobel) was used as the catalyst. Ahlstrom 42052L, multi-axial glass fiber, was used as the reinforcement material. Cerex nonwoven fabric (17 GSM) from Cerex Advanced Fabrics was used as the interleaving material. Cerex nonwoven fabrics are made by spinning and autogenously bonding continuous filaments of nylon 66 into a flat, strong fabric.

Fabrication of Composite Laminates

Metal moulds were used to manufacture the interleaved and noninterleaved composite specimens. Laminates with eight layers of glass fabrics were manufactured for the DCB tests, while laminates with six glass fabric layers were made for the

Table I. Percentage by Weight of Composite Components for Panels

Abbrev	Constituents	% Glass fiber	% Polyester resin	% Nylon veil
Short beam shear and three point bend panels				
AG	All glass layers	75.9	24.1	0
GNG	One nylon veil between each glass layer with glass layer on the outer surface	74.8	23.6	1.6
NGN	One nylon veil between each glass layer with one veil also placed on both outer surfaces	73.5	24.3	2.2
NNG	Two nylon veils between each glass layer with two veils placed on both outer surfaces	68.3	27.6	4.1
DCB panels				
AG	All glass layers	75.7	24.3	0
NGN	One nylon veil between each glass layer with one veil also placed on both outer surfaces	73.7	24.7	1.6
NNG	Two nylon veils between each glass layer with two veils placed on both outer surfaces	72.2	24.6	3.2

SBS and 3PB tests. The laminates were laid up in a cross-ply (0/90) layout and formed by compression moulding using a hydraulic press. The panels were allowed to cure at room temperature for 24 h followed by postcuring at 80°C for 3 h. Four laminate types were manufactured with varying amount and location of interleaved nylon veils. Table I shows the abbreviations used to designate each type and their respective constituent content. Veil content varied from 0% (AG) up to 4% (NNG) by weight in SBS/3PB laminates. Test specimens were cut from the manufactured laminates for characterization.

Characterization

3PB tests were carried out in accordance with ASTM D7264 on a multipurpose Tinius Olsen machine. A span-to-thickness ratio of 32 : 1 was used giving a span of 90 mm on the test fixture. Five specimens were tested from each set.

SBS testing was conducted in the same machine, with reference to ASTM D2344. A span-to-thickness ratio of 4 : 1 was used

with a span of 10 mm on the test fixture. Five specimens were tested from each set.

The gelation of liquid resin with and without nylon veils was examined at room temperature (30°C) with DMA, TA Instruments DMA Q800. A measured amount of liquid resin, mixed with the curing agent, was soaked on a support glass fabric and wrapped in an aluminium foil. Similar samples were prepared with the liquid resin soaked on a glass fabric along with one and two pieces nylon veils, respectively. The samples were subjected to DMA in dual cantilever mode at an amplitude of 20 microns for 90 min while the liquid resin progressed from a liquid to a solid state, similarly to that in Refs. 14,15. The change in complex viscosity was noted against time, which gave an indication of the start of gelation.

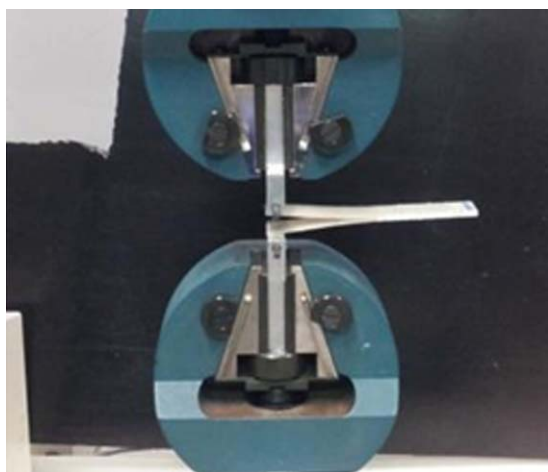


Figure 1. DCB test specimen in test rig. [Color figure can be viewed in the online issue, which is available at wileyonlinelibrary.com.]



Figure 2. DIC camera and Tinius Olsen test machine. [Color figure can be viewed in the online issue, which is available at wileyonlinelibrary.com.]

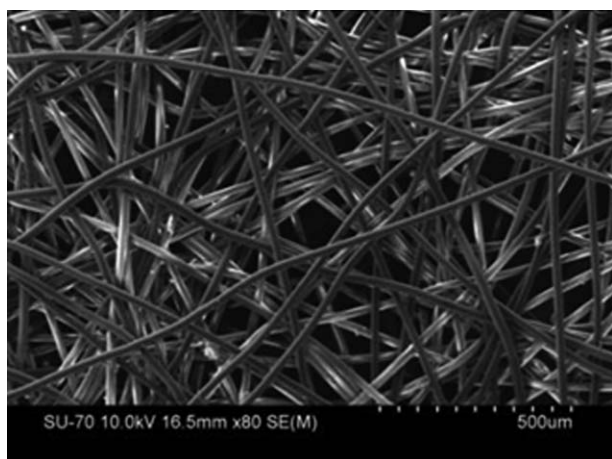


Figure 3. SEM micrograph of nylon veil.

DMA was also conducted with composite samples in accordance with ASTM D5023, using the three point bend clamp, over a temperature range from 30°C to 140°C, with a temperature increase rate of 5°C/min. An amplitude of 10 microns was applied at a frequency of 1 Hz. Five specimens were tested from each set.

The DCB testing was conducted in accordance with ASTM D5528, except for the use of a cross-ply lay-up. A cross-ply lay-up was used as it was believed that the veils could have a significant effect on fiber bridging, which is more prevalent in multi-directional laminates than unidirectional laminates, as shown by Robinson et al.¹⁶ Thus for this comparative study on the effect of having a veil or not, it was believed a cross-ply lay-up would give the best differentiation in results. Prior to testing, both sides of the test specimens were coated with a thin layer of Tipp-Ex correction fluid from the end of the PTFE insert to aid in detection of the visual onset of delamination. The specimens were then marked with thin vertical lines every 1 mm for the first 5 mm, and then every 5 mm for the remaining length of the sample. Loading blocks were used to apply the load during testing, which was carried out using a multipurpose Tinius Olsen machine with a 1 kN load cell. The specimens were mounted as shown in Figure 1 and loaded at a constant rate of 5 mm/min. The growth of the crack was tracked visually and also with the use of a LaVision two-dimensional (2D) Digital Image Correlation (DIC) camera, shown in Figure 2, with

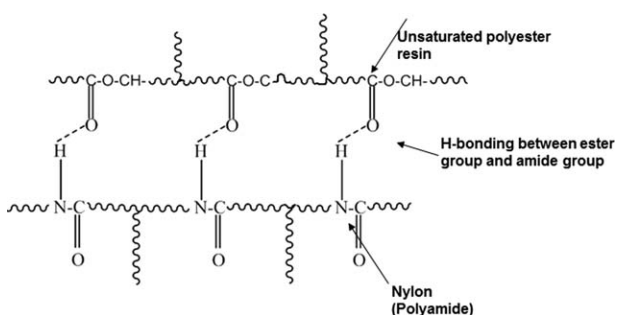


Figure 4. Schematic diagram showing potential chemical interaction between unsaturated polyester resin and nylon veil.

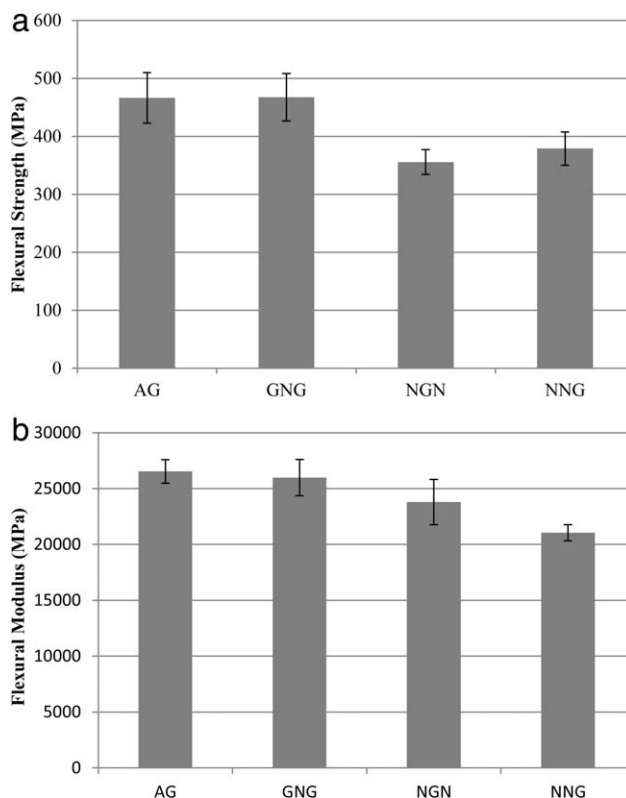


Figure 5. (a) Flexural strength and (b) flexural modulus of the composite specimens.

results analyzed via LaVis 7.4 processing software. The magnifying camera of the DIC system was focused on the edge of the specimen and linked with a load–displacement data logger. By capturing images at a fixed rate, it provided a link between the crack length in the images, the force on the specimen and the crosshead displacement at each moment. Five specimens of each type were tested.

Fracture surfaces obtained from the 3PB and DCB tests were observed using a Hitachi SU-70 Field Emission Scanning Electron Microscope (FESEM). Prior to analysis the samples were coated with a thin layer of gold, using an EMITech sputter coater for 30 s. An acceleration voltage of 5 kV was used. All

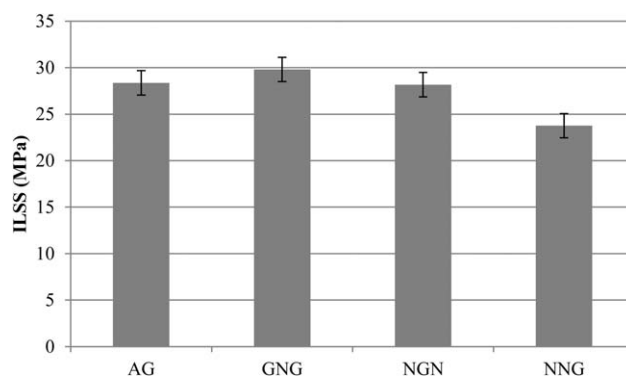


Figure 6. Interlaminar shear strength (ILSS) values of the composite specimens.

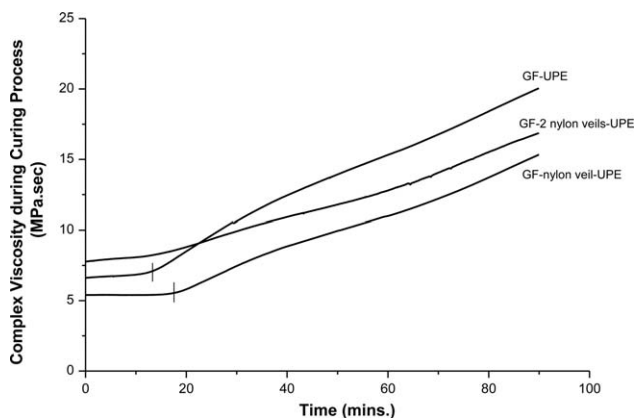


Figure 7. Change of complex viscosity of liquid resin with and without nylon veil during curing process observed against time from DMA.

images were taken at or near the point of fracture for the 3PB specimens, and on the DCB fracture surfaces of the specimens.

RESULTS AND DISCUSSION

The nylon veil was examined under SEM to measure the size of fibers (Figure 3). The fibers were approximately 25 μm in diameter and randomly distributed. The possible interaction between the nylon fibers and the unsaturated polyester resin is shown schematically in Figure 4. H-bonding between the amide groups of the nylon veil and the ester groups of the unsaturated polyester resin molecule can ensure good chemical interaction between them, improving the properties.

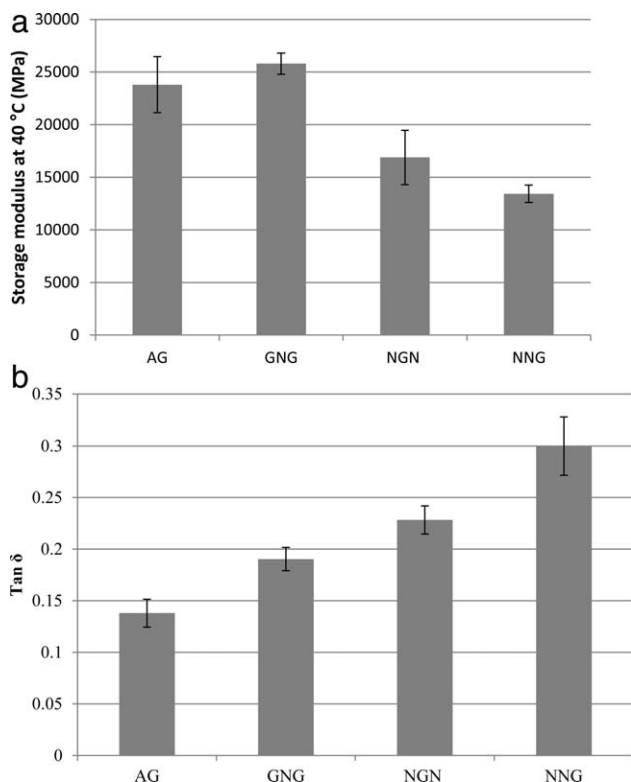


Figure 8. (a) Storage modulus and (b) damping parameter of the composite specimens.

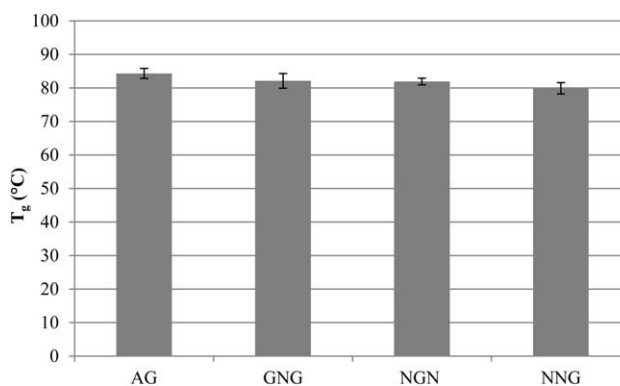


Figure 9. Glass transition temperature (T_g) of the composite specimens measured from the peak of loss modulus curves.

The flexural strength and modulus of all the composite laminates are shown in Figure 5(a,b) respectively. Note that actual specimen thickness was used to convert force to stress, although it was actually found that the veils had negligible effect on consolidated specimen thickness. The flexural strength was almost the same for AG and GNG samples (466 and 467.5 MPa, respectively), while reduced flexural strength was found for NGN and NNG samples (355.6 and 378.9, MPa respectively). The flexural modulus of AG, GNG, NGN, and NNG samples were found to be 26.5, 26, 23.8, and 21 GPa, respectively. We see for example, that a doubling of the nylon content from the NGN to the NNG samples resulted in an 11.5% decrease in flexural modulus. This reduction in stiffness results from a more compliant interlaminar region, as described later.

SBS tests were carried out to determine the apparent interlaminar shear strength (ILSS) of the manufactured specimens. ILSS values, shown in Figure 6, were found to be very similar in the

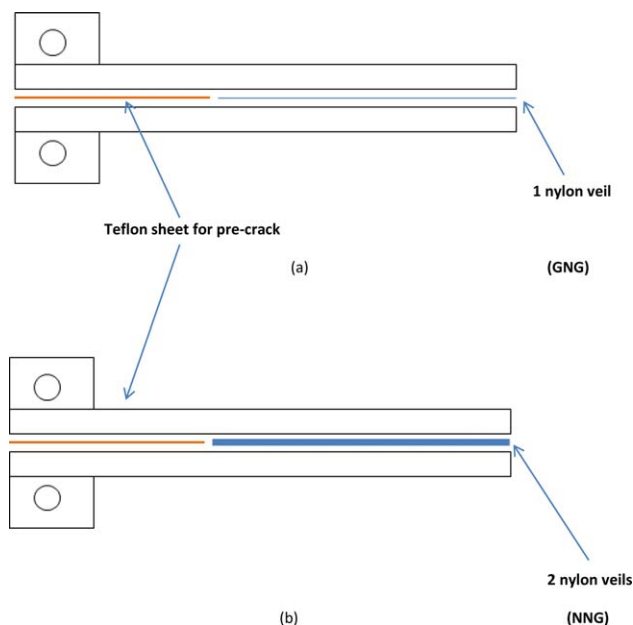


Figure 10. Schematic diagram of DCB test specimen containing (a) one (GNG) and (b) two (NNG) nylon veils. [Color figure can be viewed in the online issue, which is available at wileyonlinelibrary.com.]

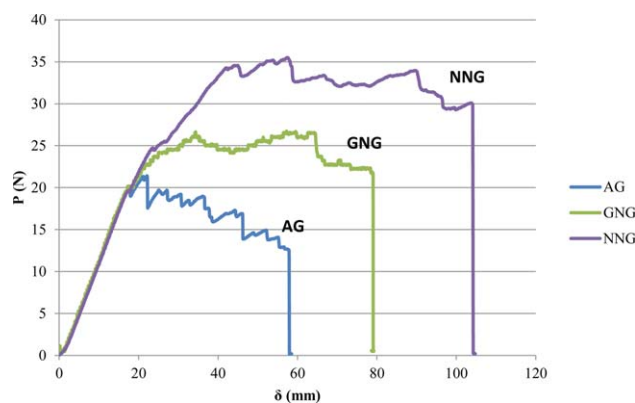


Figure 11. Load vs displacement curves of the composite specimens under DCB test. [Color figure can be viewed in the online issue, which is available at wileyonlinelibrary.com.]

AG, NGN, and GNG samples, but there was a drop of 16% in the NNG samples compared to that of the AG samples. The ILSS is influenced by the chemical interaction of the nylon veil with the resin at the interface. It is likely that the hydrogen bonding between the amide groups of nylon and the ester groups of unsaturated polyester resin (shown in Figure 4) helped the composites to retain their ILSS values. However, with the presence of two layers of nylon, a lower percentage of the nylon veils would be in intimate contact with the resin, reducing the hydrogen bonding effect, which may explain the afore-mentioned 16% drop in ILSS.

As noted above, the gelation behavior of the resin with and without nylon veil was monitored at room temperature with DMA. The change in complex viscosity of the liquid resin during the curing process with and without nylon veil is shown in Figure 7. The point of increase of complex viscosity was considered as the gel point of the resin. The complex viscosity began to rise after 12 min for the UPE resin, whereas for the UPE resin with one nylon veil, the rise in complex viscosity was observed after 20 min. With two nylon veils, there was a gradual increase in the complex viscosity indicating a delayed gelation. This observation indicates that the processing of such interleaved composites may be facilitated by the presence of nylon veils as the veils would slightly delay the gelation process allowing more time for resin flow and fiber wetting.

The results from DMA of the composites over a temperature range from 30°C to 140°C are shown in Figure 8. The variation in storage modulus as a function of temperature is shown in Figure 8(a). An increase in storage modulus was noted for the GNG samples at room temperature compared to that of AG samples. However, the overall trend was a decline in storage modulus as more nylon veils were added. There was a 29% reduction in storage modulus between the AG panel and the NGN panel. The highest reduction was noted for the NNG panel which displayed a storage modulus almost 45% lower than the AG panel. This result is consistent with the stiffness trends in the 3PB tests. The peak damping parameter ($\tan \delta$) values showed a clear upward trend with nylon content, as seen in Figure 8(b). Relative to the baseline value for the AG panel, there was a 117% increase in $\tan \delta$ for the NNG panel. An

increase of 38% occurred between the AG and GNG panels, which implies that the presence of nylon veils in the composite, even in the lowest concentration, had a significant positive effect on the damping ability of the material. A small rise in peak $\tan \delta$ was observed between the GNG and NGN panels (20%), demonstrating the positive effect of adding nylon veils to the material surface.

The variation in glass transition temperature, T_g , is shown in Figure 9. The addition of nylon veils had little effect on the T_g with the highest concentration of nylon (NNG panel) resulting in a drop in T_g of just 5%. The chemical interaction between the nylon veil fibers and the resin molecules most likely helped to retain the T_g . The almost constant value of T_g with increasing nylon veil content indicates that despite the effects of nylon on storage modulus, it did not affect acceptable service temperature of the composite, compared to the baseline noninterleaved composite.

The AG, GNG, and NNG panels were subjected to DCB testing. NGN samples were not subjected to DCB test as both GNG and NGN samples contained one nylon veil at the crack propagating plane, and hence will give similar results. A schematic diagram showing one and two nylon veils at the crack propagating planes of GNG and NNG samples, respectively, is shown in Figure 10(a,b), respectively. Figure 11 shows the load versus displacement behavior of the composite samples under DCB test. The samples containing nylon veils withstood a much higher load and exhibited a greater displacement until complete failure. The average maximum force increased by 25% and 65.8% for GNG and NNG samples respectively, in comparison to the AG samples. The displacement to fracture for the GNG and NNG samples were respectively 36% and 79% higher compared to that of AG samples. The AG samples showed a number of distinct sudden drops in load which corresponded with abrupt jumps in crack length. The samples with added nylon veils, regardless of nylon content, exhibited smoother crack propagation. The smooth load–displacement curves of the nylon veil interleaved samples are indicative of more stable crack propagation in these composites.

The critical strain energy release rate, G_{IC} , for each set of composites is shown in Figure 12. The value of G_{IC} increased with increasing nylon veil content. The average value of G_{IC} for GNG

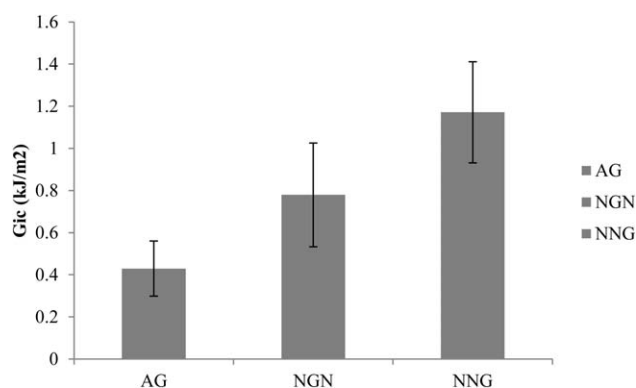


Figure 12. G_{IC} values of the composite samples obtained from DCB testing.

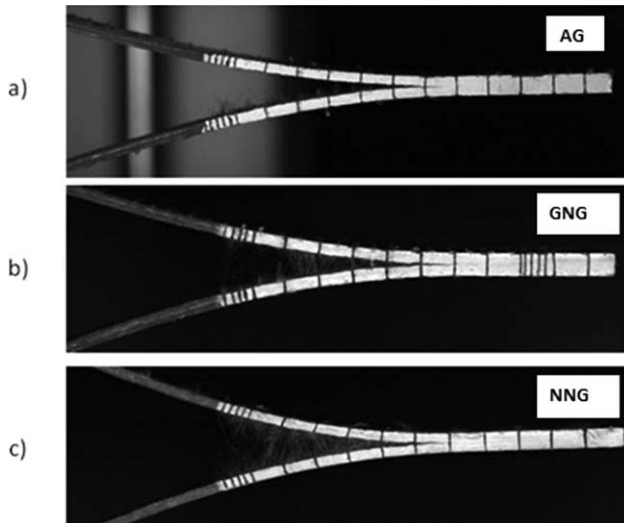


Figure 13. Images from DIC camera indicating fiber bridging in interleaved samples.

and NNG specimens was found to be 80% and 170% higher, respectively, than that for the baseline AG specimens.

Some insight into these effects of nylon veils can be obtained from pictures of the interleaved samples during the DCB test, as shown in Figure 13. It can be seen that as the crack length grew, a significant amount of fiber bridging was observed in both GNG and NNG samples. It is well known that fiber bridging plays a major role in interlaminar toughness. The AG sample had almost no evidence of fiber bridging. Pullout and breakage of the ductile nylon fibers absorbs a large amount of energy and increases the G_{IC} value of the material. The pulled out fibers close to the delamination front also provide resistance to crack growth, delivering further energy absorption. The increase in G_{IC} observed here is in agreement with the increase reported by Yasae et al.,¹² who used interleaving thermoplastic films and chopped fibers in a glass fiber/epoxy composite. In their case, the increase in G_{IC} was because of the energy required to peel the films from the epoxy and break the chopped fibers during crack propagation, which is somewhat

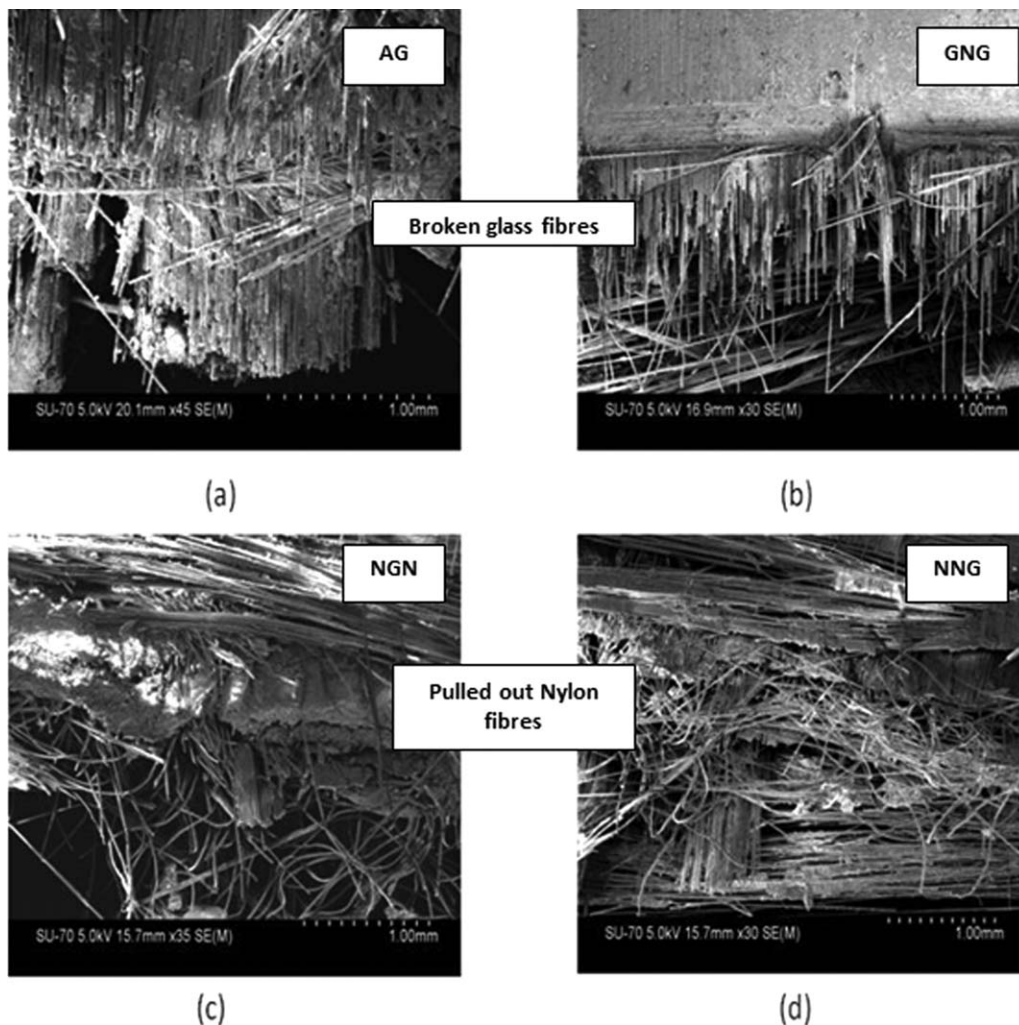


Figure 14. Fracture surfaces from 3PB testing viewed with SEM.

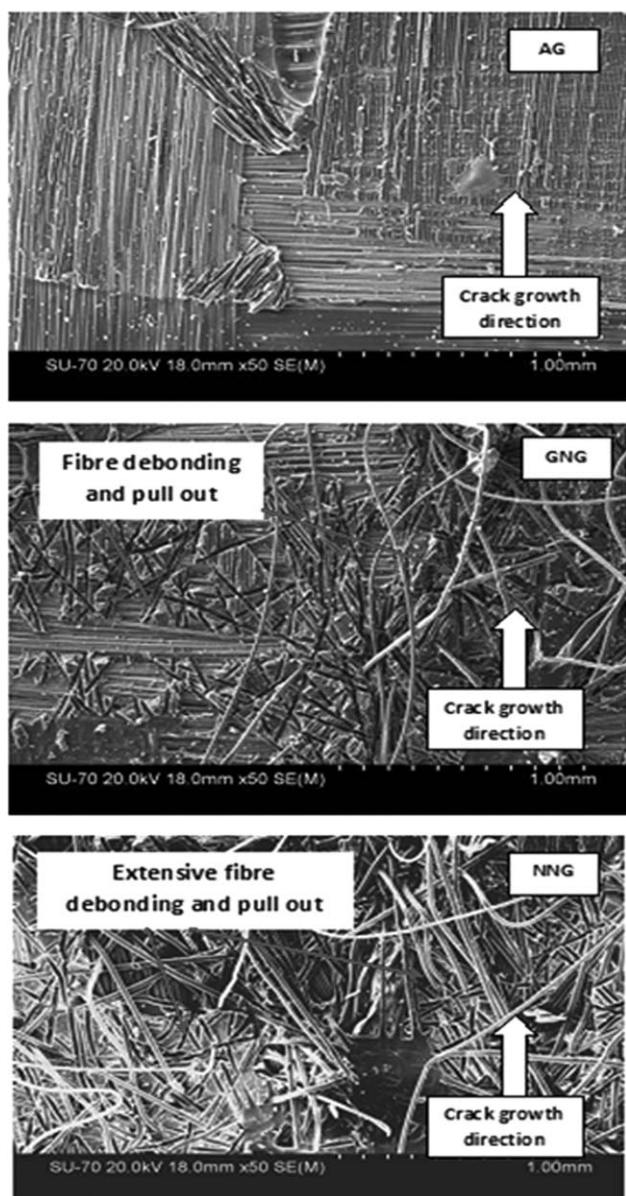


Figure 15. SEM micrograph of the DCB fracture surface.

different from the mechanism here. The G_{IC} values for the baseline AG samples are also in line with those found by Yasae et al.¹²

SEM images of the fracture surfaces from the 3PB tests are shown in Figure 14. An increasing level of disorder is evident in the fracture surfaces with increasing nylon content, i.e. from GNG to NGN to NNG samples [depicted in Figure 14(b–d)], which is because of pull out of the fibers from the nylon veils. The DCB fracture surfaces are shown in Figure 15. The AG sample showed a clean DCB fracture surface while nylon fiber debonding and pull-out was evident in the GNG sample and even more so in the NNG sample. The debonding and pulling out of the nylon fibers from the matrix during the propagation of the crack is likely to play a dominant role in the increased G_{IC} values seen for nylon-interleaved samples. The increase in fiber bridging and resulting G_{IC} values in this study provides

evidence of the usefulness of this interleaving veil approach in the improvement of interlaminar toughness of glass fiber reinforced, unsaturated low-styrene emission polyester resin composites. This technique thus shows promise for low-cost materials used in industrial applications.

CONCLUSIONS

Incorporation of nylon veils as interleaving materials in glass fiber reinforced, unsaturated low-styrene emission polyester resin composites resulted in a significant improvement in damping properties. The damping parameter increased by 117% in comparison to the all glass fiber reinforced composites when two layers of nylon veils were inserted as interleaving materials. The DCB test results showed increasing nylon veil content correlated with increasing mode-I interlaminar toughness, characterized by critical strain energy release rate, G_{IC} . The sample containing two layers of nylon veils between each glass layer exhibited an increase of up to 170% in G_{IC} over the values obtained for the all glass fiber/unsaturated polyester resin composite. This significant increase was attributable to the high extent of fiber bridging as the nylon fibers were debonded and pulled out from the matrix. The pulling out of these fibers from the matrix, and their subsequent breakage, absorbed energy and toughened the interlaminar region of the composite. The test results indicated that the negative impact of nylon on certain properties such as flexural modulus and interlaminar shear strength were outweighed by the positive impact on the critical strain energy release rate for mode-I fracture (G_{IC}) and damping parameter, particularly for energy-absorbing applications. The interleaving technique presented has potential health and safety benefits, as it can widen the possible applications for relatively brittle low styrene emission unsaturated polyester resin composites.

ACKNOWLEDGMENTS

The authors wish to acknowledge the Irish Centre for Composites Research, funded by Enterprise Ireland and the Industrial Development Agency of Ireland, under the Technology Centre programme for financial support; Scott Bader for supplying the resin Crystic 2-446PA and the initiator Butanox LPT-IN; Cerex Advanced Fabrics for supplying the Cerex interleaving nylon fabrics (17 gsm); and Mr. Jamie OSullivan of the Civil Engineering and Materials Science Department and Mr. Adrian McEvoy of the Department of Mechanical, Aeronautical and Biomedical Engineering at the University of Limerick for their useful suggestions.

REFERENCES

- Pegoretti, A.; Cristelli, I.; Migliaresi, C. *Compos. Sci. Technol.* **2010**, *68*, 2653.
- Hong, S.; Liu, D. *Exp. Mech.* **1989**, *29*, 115.
- Lear, M. H.; Sankar, B. V. *J. Mater. Sci.* **1999**, *34*, 4181.
- Baley, C.; Perroti, Y.; Davies, P.; Baourmaud, A.; Grohens, Y. *Appl. Comp. Math.* **2006**, *13*, 1.
- Perrot, Y.; Baley, C.; Grohens, Y.; Davies, P. *Appl. Comp. Math.* **2007**, *14*, 67.

6. Lee, S. H.; Lee, J. H.; Cheong, S. K.; Noguchi, H. *J. Mater. Process. Technol.* **2008**, *207*, 21.
7. Kuwata, M.; Hogg, P. J. *Compos. Part A* **2011**, *42*, 1551.
8. Kuwata, M.; Hogg, P. J. *Compos. Part A* **2011**, *42*, 1560.
9. Hamer, S.; Leibovich, H.; Green, A.; Intrater, R.; Avrahami, R.; Zussman, E.; Siegmann, A.; Sherman, D. *Polym. Compos.* **2011**, *32*, 1781.
10. Tzetzis, D.; Hogg, P. J. *Compos. Part A* **2006**, *37*, 1239.
11. Tzetzis, D.; Hogg, P. J. *Mater. Technol.* **2007**, *22*, 2.
12. Yasae, M.; Bond, I. P.; Trask, R. S.; Greenhalgh, E. S. *Compos. Part A* **2012**, *43*, 198.
13. Yasae, M.; Bond, I. P.; Trask, R. S.; Greenhalgh, E. S. *Compos. Part A* **2012**, *43*, 121.
14. Kim, M. G.; Nieh, W. L. S.; Meacham, R. M. *Ind. Eng. Chem. Res.* **1991**, *30*, 798.
15. Lorenz, L. F.; Christiansen, A. W. *Ind. Eng. Chem. Res.* **1995**, *34*, 4520.
16. Robinson, P.; Song, D. Q. *J. Comp. Mater.* **1992**, *26*, 1554.